Dynamics of Membrane Adhesion: The Role of Polyethylene Glycol Spacers, Ligand−Receptor Bond Strength, and Rupture Pathway†

Joyce Y. Wong*,‡ and Tonya L. Kuhl*,§

Department of Biomedical Engineering, Boston University, 44 Cummington Street, Boston, Massachusetts 02215, and Departments of Chemical Engineering and Materials Science and Biomedical Engineering, University of California−Davis, Davis, California 95616

Received August 1, 2007. In Final Form: November 15, 2007

Biological adhesion typically occurs through discrete cross bridges between complementary molecules on adjacent membranes. Here we report quantitative measurements of the binding distance between a lipid membrane functionalized with ligands on flexible polymer tether chains and a second membrane bearing complementary receptors using the surface force apparatus technique. The binding distance is shown to increase as a function of polymer tether length. Upon separation, adhesive failure occurs not at the strong ligand−receptor bond but primarily through the mechanical pullout of cross-bridging polymer tethers from the membrane. We summarize these measurements of complementary membrane adhesion dynamics using an energy-state diagram that encompasses the energetics of the polymer tether, ligand−receptor bond strength, and number of cross bridges formed.

I. Introduction

Cellular processes are governed by dynamic receptor−ligand interactions.[1] For instance, the response of the immune system to infection involves the attachment and migration of patrolling cells of the circulating blood and lymph through tissues.[2] Processes such as cell spreading and locomotion are facilitated by coordinated attachment−detachment sequences that underlie processes such as tissue morphogenesis.[3] An elucidation of the relationships between the range of attraction between a given ligand−receptor pair and the time required to bind is therefore crucial to our understanding of adhesion mechanisms. This knowledge would also significantly advance our ability to design biomimetic materials with tunable adhesivity for tissue engineering and targeted delivery of therapeutic/diagnostic agents.[4−7]

Cell adhesion molecules (CAMs) are frequently anchored to cellular membranes by semiflexible repeating spacer groups. An important role of the spacer is to enable the active domain of the CAM molecule to protrude through the cell's glycocalyx to access complementary binding domains on opposing surfaces.[7−9] The spatial and temporal specificity that is a hallmark of cellular adhesion arises from a combination of background, nonspecific steric repulsive forces due to the glycocalyx long-range sampling ability conferred by the flexible tether and short-range "lock-and-key" binding. Poly(ethylene glycol) (PEG) has been used extensively as a synthetic flexible spacer that mimics the glycocalyx and CAMs: the unmodified PEG acts as a steric stabilizer,[10,11] and adhesive groups (ligands) can be easily coupled to its terminal end.[12] Although there have been numerous studies investigating the steric effects of PEG, a complete understanding of its unique behavior is still lacking. Moreover, whereas many studies utilize PEG as a tether for attaching ligands, few studies have directly investigated the role of the PEG tether in membrane adhesion and separation.[13]

Using the well-characterized ligand−receptor pair biotin−streptavidin, a few studies have mapped the adhesion dynamics between surfaces cross linked via functionalized poly(ethylene glycol) (PEG) tethers.[14−17] The mechanisms of detachment of these adherent surfaces involve the rupture of discrete complementary bonds and the mechanical detachment of cross linkers from the membrane surface. In contrast to adhesion measurements, there is a paucity of information available on the dynamics of the initial binding event. Recently, there have been efforts to expand laminar flow chamber experiments, which have been used extensively to quantify adhesion under controlled hydrodynamic flow[4] in order to provide information on the distances and rates of particle attachment through ligand−receptor recognition.[18] By carefully monitoring particle velocities in well-defined flow fields coupled with theoretical simulations, the distance of a particle from a complementary surface just prior to a binding event can be monitored with a distance resolution on the order of 10 nm. In contrast, higher-resolution measurements of binding distances are primarily the domain of surface force apparatus (SFA) measurements, where the separation distance

† Part of the Molecular and Surface Forces special issue.

* E-mail: jywong@bu.edu, tlkuhl@ucdavis.edu.

‡ Boston University.

§ University of California−Davis.

(1) Hammer, D. A.; Tirrell, M. *Annu. Rev. Mater. Sci.* **1996**, 26, 651−691.
(2) Springer, T. A. *Nature* **1990**, *346*, 425−434.
(3) Clark, E. A.; Brugge, J. S. *Science* **1995**, *268*, 233−239.
(4) Bongrand, P. *Rep. Prog. Phys.* **1999**, *62*, 921−968.
(5) Leckband, D.; Israelachvili, J. *Q. Rev. Biophys.* **2001**, *34*, 105−267.
(6) Dillow, A. K.; Tirrell, M. *Curr. Opin. Solid State Mater. Sci.* **1998**, *3*, 252−259.
(7) Johnson, C. P.; Fujimoto, I.; Perrin-Tricaud, C.; Rutishauser, U.; Leckband, D. *Proc. Natl. Acad. Sci. U.S.A.* **2004**, *101*, 6963−6968.
(8) Patel, K. D.; Moore, K. L.; Nollert, M. U.; Mcever, R. P. *J. Clin. Invest.* **1995**, *96*, 1887−1896.
(9) Sivasankar, S.; Gumbiner, B.; Leckband, D. *Biophys. J.* **2001**, *80*, 1758−1768.
(10) Harris, J. M. *Poly(ethylene glycol) Chemistry: Biotechnical and Biomedical Applications*; Plenum Press: New York, 1992.
(11) Napper, D. H. *Polymeric Stabilization of Colloidal Dispersions*; Academic Press: London, 1983.
(12) Zalipsky, S.; Mullah, N.; Qazen, M. *Methods Enzymol.* **2004**, 387, 50−69.
(13) Ratto, T. V.; Langry, K. C.; Rudd, R. E.; Balhorn, R. L.; Allen, M. J.; McElfresh, M. W. *Biophys. J.* **2004**, *86*, 2430−2437.
(14) Wong, J. Y.; Kuhl, T. L.; Israelachvili, J. N.; Mullah, N.; Zalipsky, S. *Science* **1997**, *275*, 820−822.
(15) Lin, J. J.; Silas, J. A.; Bermudez, H.; Milam, V. T.; Bates, F. S.; Hammer, D. A. *Langmuir* **2004**, *20*, 5493−5500.
(16) Kim, D. H.; Klibanov, A. L.; Needham, D. *Langmuir* **2000**, *16*, 2808−2817.
(17) Jeppesen, C.; Wong, J. Y.; Kuhl, T. L.; Israelachvili, J. N.; Mullah, N.; Zalipsky, S.; Marques, C. M. *Science* **2001**, *293*, 465−468.
(18) Pierres, A.; Benoliel, A. M.; Zhu, C.; Bongrand, P. *Biophys. J.* **2001**, *81*, 25−42.

10.1021/la702357a CCC: $40.75
Published on Web 01/11/2008

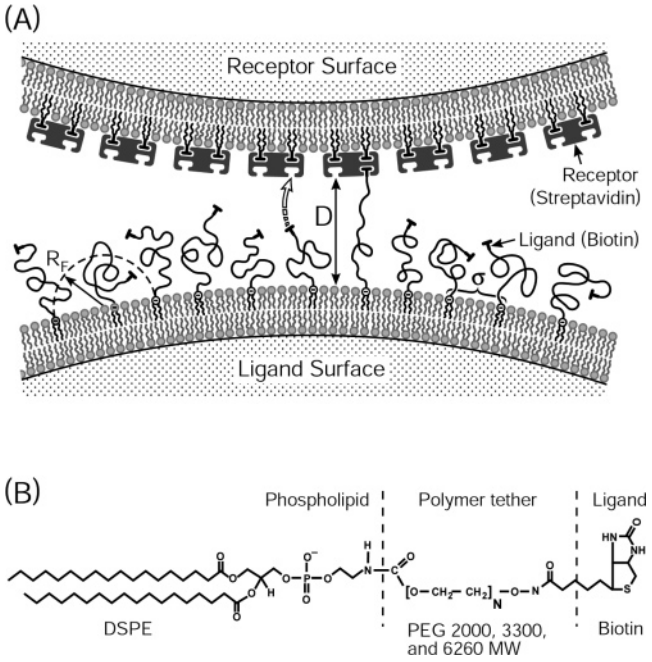

Figure 1. (A) Schematic illustration of the complementary ligand and receptor membranes used in the SFA experiments. The functionalized polymer tether coverage is $\sigma = 950$ Å^2/molecule or 4.5 mol % of the outer membrane leaflet. A monolayer of streptavidin is presented on the opposing membrane surface. The length of the tether, density of ligands and receptors, and phase state of the membranes can be controlled independently. (B) Structure of functionalized phospholipid DSPE−PEG_{MW}−biotin. The length of the PEG chain was varied from 2000 to 3300 to 6260 MW.

between functionalized membrane surfaces can be controlled and directly measured with 0.2 nm resolution.[19]

Here, we specifically address the effect of tether length and ligand−receptor bond strength on controlling the spatial dependence of complementary membrane−membrane adhesion. We use the SFA technique to obtain quantitative measurements of the binding distance between lipid membranes functionalized with poly(ethylene glycol) (PEG)-tethered biotin and an opposing membrane bearing the complementary receptor, streptavidin (Figure 1). This approach is in contrast to binding kinetic studies where ligands or receptors freely diffuse in solution or when the ligands are immobilized directly at the membrane surface (i.e., without a flexible spacer[20,21]). A key physical property of tethering chains is that they are not static but sample a distribution of conformations. Consequently, the interaction between membrane-tethered ligands and receptors is greatly modified by the dynamic sampling of the tethering chain. Moreover, we have shown previously that the range of binding cannot be predicted from the equilibrium or average conformation of the tethering chain but depends specifically on the dynamic spatial sampling of the tether and the strength of the complementary binding pair.[14,17,22−24]

Our approach also directly addresses the design and tailoring of stealth liposomes for targeted drug delivery. Stealth liposomes have a protective end-grafted polymer tether coating of poly(ethylene glycol) (PEG) that prevents the nonspecific adsorption of proteins and significantly increases their in vivo circulation time.[25−35] To develop effective targeting vehicles for the delivery of highly toxic drugs such as chemotherapy agents, biospecific molecules (e.g., ligands) must be available at the distal region of the protective polymeric coating to provide cellular specificity. Although efficient targeting is highly desirable, nonspecific protein adsorption must still be minimized to maintain reasonable circulation times. To satisfy each of these two criteria, one must achieve the appropriate balance between nonspecific and specific interactions. To date, the most efficacious structure for the polymeric coating remains an open question.[36,37]

II. Materials and Methods

1. Materials. High-purity dipalmitoyl phosphatidyl ethanolamine (DPPE), dilauroyl phosphatidyl ethanolamine (DLPE), and distearoyl phosphatidyl ethanolamine were purchased from Avanti Polar Lipids Inc. (Alabaster, AL) in powder form. *N*-((6-(Biotinoyl)amino)-hexanoyl)-1,2-dihexadecanoyl-*sn*-glycero-3- phosphoethanolamine, triethylammonium salt (biotin−X−DHPE, where X is a six-carbon spacer) was purchased from Molecular Probes (Eugene, OR). Streptavidin was purchased from Boehringer-Mannheim (Indianapolis, IN). All salts were high purity (>99.5%) and were purchased from Sigma-Aldrich (St. Louis, MO). Water was purified with a Millipore Milli-Q UV filtration system (Billerica, MA). HPLC-grade methanol and chloroform were from Mallinckrodt (St. Louis, MO). PEG lipids (Figure 1B) were prepared as described previously.[12,38] The PEG tether MW in these experiments was 2000, 3300, or 6260 ($N = 44$, 77, or 142 monomer units, respectively).[14,17]

2. Ligand−Receptor Pair. The strong affinity ligand−receptor pair biotin−streptavidin was utilized in these studies (binding constant of 88 kJ/mol or ∼35*kT*/bond).[39−42] Biotin−streptavidin is one of the most thoroughly studied and characterized ligand−receptor systems and is used ubiquitously in biotechnological applications. Streptavidin has four identical biotin binding sites and a two-fold axis of symmetry, where two pairs of biotin binding sites lie on two opposing faces of the protein.[43] By incorporating biotin−X−DHPE at a defined molar ratio into a membrane (receptor surface), an oriented membrane-bound monolayer of streptavidin can easily be formed by subsequently absorbing streptavidin from solution (described below).[40,42] Thus, two of the biotin binding sites immobilize and orient the streptavidin molecule, forming the receptor surface (Figure 1). The other two binding sites are then available for binding with the opposing ligand surface. Such control over the density and orientation of receptors is crucial for quantitative studies.

(19) Israelachvili, J. N.; Adams, G. E. *J. Chem. Soc., Faraday Trans. 1* **1978**, 74, 975−1001.
(20) Pierres, A.; Benoliel, A. M.; Bongrand, P. *J. Phys. III* **1996**, *6*, 807−824.
(21) Bell, G. I. *Science* **1978**, *200*, 618−627.
(22) Moreira, A. G.; Marques, C. M. *J. Chem. Phys.* **2004**, *120*, 6229−6237.
(23) Moreira, A. G.; Jeppesen, C.; Tanaka, F.; Marques, C. M. *Europhys. Lett.* **2003**, *62*, 876−882.
(24) Carignano, M. A.; Szleifer, I. *Interface Sci.* **2003**, *11*, 187−197.
(25) Lasic, D. D.; Macleod, K.; Huang, A.; Abra, R. M.; Newman, M. S.; Martin, F. J.; Needham, D.; Mayhew, E. *Abstr. Pap. Am. Chem. Soc.* **1992**, *203*, 51-Biot.
(26) Lasic, D. D., *Angew. Chem., Int. Ed. Engl.* **1994**, *33*, 1685−1698.
(27) Woodle, M. C.; Lasic, D. D. *Biochim. Biophys. Acta* **1992**, *1113*, 171−199.
(28) Ceh, B.; Lasic, D. D. *J. Colloid Interface Sci.* **1997**, *185*, 9−18.
(29) Torchilin, V. P.; Trubetskoy, V. S. *Adv. Drug Delivery Rev.* **1995**, *16*, 141−155.
(30) Klibanov, A. L.; Maruyama, K.; Torchilin, V. P.; Huang, L. *FEBS Lett.* **1990**, *268*, 235−237.
(31) Torchilin, V. P.; Omelyanenko, V. G.; Papisov, M. I.; Bogdanov, A. A.; Trubetskoy, V. S.; Herron, J. N.; Gentry, C. A. *Biochim. Biophys. Acta* **1994**, *1195*, 11−20.
(32) Woodle, M. C. *Adv. Drug Delivery Rev.* **1998**, *32*, 139−152.
(33) Lasic, D. D.; Needham, D. *Chem. Rev.* **1995**, *95*, 2601−2628.
(34) Kuhl, T. L.; Leckband, D. E.; Lasic, D. D.; Israelachvili, J. N. *Biophys. J.* **1994**, *66*, 1479−1488.
(35) Kenworthy, A. K.; Hristova, K.; Needham, D.; Mcintosh, T. J. *Biophys. J.* **1995**, *68*, 1921−1936.
(36) Torchilin, V. P. *Nat. Rev. Drug Discovery* **2005**, *4*, 145−160.
(37) Satulovsky, J.; Carignano, M. A.; Szleifer, I. *Proc. Natl. Acad. Sci. U.S.A.* **2000**, *97*, 9037−9041.
(38) Zalipsky, S. *Adv. Drug Delivery Rev.* **1995**, *16*, 157−182.
(39) Florin, E. L.; Moy, V. T.; Gaub, H. E. *Science* **1994**, *264*, 415−417.
(40) Helm, C. A.; Knoll, W.; Israelachvili, J. N. *Proc. Natl. Acad. Sci. U.S.A.* **1991**, *88*, 8169−8173.
(41) Yuan, C. B.; Chen, A.; Kolb, P.; Moy, V. T. *Biochemistry* **2000**, *39*, 10219−10223.
(42) Leckband, D.; Muller, W.; Schmitt, F. J.; Ringsdorf, H. *Biophys. J.* **1995**, *69*, 1162−1169.
(43) Green, N. M. *Methods Enzymol.* **1990**, *184*, 51−67.

Although biotin and streptavidin are not cellular adhesion molecules, they are naturally occurring biological ligand receptors and behave similarly to other ligand−receptor pairs.[5,44] Importantly, the high binding affinity of this pair is ideal for studies on the effect of flexible tethers in ligand−receptor binding and complementary adhesion because the off-rate or unbinding is minimized. Likewise, the small size of biotin (MW = 244 Da) is less likely to perturb the sampling of the polymer tether chains. Commonly used targeting ligands such as folic acid (MW = 441 Da) or the GRGDSP motif of fibronectin (MW = 588 Da) also have relatively low molecular weights.[36] Finally, the biotinylation of biomolecules is standard, and the streptavidin−biotin system is used extensively to couple antibodies[45] to targeting vehicles.

3. Substrate Preparation. Supported lipid bilayers were prepared by Langmuir−Blodgett deposition (LB) using a temperature-controlled Wilhelmy trough (Joyce-Loebl Co., Malden, MA) as described elsewhere.[34] All preparations were carried out in a laminar flow box (Labconco, Kansas City, MO). Lipids were dissolved in 9:1 chloroform/methanol to a concentration of approximately 1 mg/mL. The receptor and ligand surfaces were assembled onto molecularly smooth, back-silvered mica substrates glued onto silica disks (Figure 1). A close-packed, solid-phase inner monolayer of DPPE (∼43 Å/molecule, Π = 39 mN/m) was first deposited by pulling the substrates up through a compressed DPPE monolayer at the air−water interface. For the tethered ligand surface, a mixture of DSPE and biotin−PEG−DSPE was then deposited by passing the DPPE-coated substrates down through the monolayer film (∼43 Å/molecule, Π = 43 mN/m) to form the outer leaflet of the membrane. Subsequently, the biomembrane-coated surfaces were kept under water and mounted in the SFA. The PEG−biotin coverage was 4.5 mol % for all tether lengths, which corresponds to the so-called "weakly overlapping mushroom regime" with a density of 1.05×10^{17} m^{-2} or 950 $Å^2$ for each tethered biotin molecule.

The preparation of oriented monolayers of streptavidin has been described previously.[40,46] Briefly, streptavidin was assembled by specific adsorption onto a supported lipid bilayer with an outer leaflet consisting of a mixture of DLPE and 5 mol % DHPE−X−biotin (∼43 Å/molecule, Π = 35 mN/m). After deposition of the mixed DLPE/DHPE−X−biotin outer leaflet, the membrane was kept under water during removal from the trough and incubated with streptavidin at a concentration of 0.05 mg/mL in phosphate buffer for a minimum of 1 h. The coverage of streptavidin using this adsorption method has previously been determined to be ∼3600 $Å^2$/streptavidin, or 79% of the bilayer surface.[47]

4. Force−Distance Measurements. The surface forces apparatus (SFA) technique has been previously described[19,48] and has been used extensively to measure interaction forces between surfaces. A Mark II SFA was utilized in these studies. The substrates were molecularly smooth, back-silvered mica glued onto two cylindrically curved silica disks. The upper surface was mounted on a fixed support or piezo, whereas the lower surface was mounted on a double-cantilever spring, displaceable vertically by a micrometer screw. Light directed normally through the surfaces is partially transmitted through the silver layer on each disk and also undergoes constructive interference to produce fringes of equal chromatic order (FECO). These FECO fringes can be displayed in a spectrometer, and the distances between the surfaces can be measured by measuring fringe displacement.[48,49] The lower surface was mounted on a spring with a calibrated spring constant, which ranged from 2 to 4×10^5 mN/m. Forces were measured through deflection of this spring. When the gradient of the interaction force exceeds the spring constant of the measuring spring in the SFA, the surfaces will either jump into or out of contact. The measured radius of curvature for each contact position was used to normalize the measured force profile to enable quantitative comparison between different contact positions and experiments. The Derjaguin approximation gives the relationship between the interaction energy per unit area for two flat plates and the force−distance relationship between two crossed cylinders

$$E(D) = \frac{F(D)}{2\pi R} \tag{1}$$

where E is the energy per unit area, F is the force between the cylinders, R is the radius of the contact position, and D is the separation distance.[50] The Derjaguin approximation is valid at small distances where $D \ll R$. The radius of curvature was measured for two cross sections at 90°, and the geometrical mean was used in calculations. For these experiments, the radius of curvature was 1.0 ± 0.5 cm.

In the force−distance curves shown in this study, D was defined as the distance between the outer edge of the streptavidin-functionalized supported lipid bilayer (receptor surface) and the outer lipid head group surface on the opposing surface (ligand surface) (Figure 1A). This reference frame was determined at the end of each experiment by draining the buffer from the SFA with the surfaces well separated. This process removes the outer monolayers of the assembled bilayers. The total thickness change after draining is the sum of the material removed with the outer monolayers. The absolute position of D was established by accounting for the thicknesses of the various layers, DSPE, DLPE, and streptavidin with the remainder ascribed to the PEG tether chains. All SFA measurements were conducted in phosphate buffer containing 0.5 mM Na^+ at pH 7.2. The lateral diffusion of lipids was minimized by operating at 25 ± 0.2 °C, which is below the phase-transition temperature of the lipid bilayers.

III. Results

1. Binding Distance. The measured force−distance relationship between a ligand and receptor surface is quite different for the PEG-tethered biotin case compared to that of the untethered biotin (Figure 2A). When the ligand and receptor are both rigidly bound to their respective surfaces, the ligand−receptor interaction is intrinsically very short-ranged (<5 Å) (Figure 2A, dashed curve).[40,42] Conversely, with the ligand attached to the end of a polymer tether, there is a large attractive force whose binding range, d_B, is much larger than the equilibrium or average extension of the tether chain given by the Flory radius of a chain under good solvent conditions

$$R_F = aN^{3/5} \tag{2}$$

where a is the length of a monomer ([−CH_2CH_2O−] ≈ 3.5 Å) and N is the number of monomers in the tether chain. This observation indicates that even though the higher-energy, extended conformations (distances) are less frequent (e.g., Boltzmann-weighted) this highly dynamic sampling allows the ligated end to bind to complementary receptors at greatly increased distances.[14,17,24] For tether conformations in which the ligand (biotin) is less than 5 Å from a streptavidin binding site, the specific short-range interaction can lock-in, pinning the chain to the opposing surface. When the "bound" polymer tethers are highly stretched, the resulting tension acts as a restoring force to bring the surfaces closer together, thereby allowing more energetically favorable conformations. Interestingly, only a few chains need to bridge to trigger the adhesion event. This point is discussed in more detail below, but essentially, the interaction potential between opposing ligand and receptor surfaces is

(44) Vijayendran, R.; Hammer, D.; Leckband, D. *J. Chem. Phys.* **1998**, *108*, 7783−7794.
(45) Sakhalkar, H. S.; Dalal, M. K.; Salem, A. K.; Ansari, R.; Fu, J.; Kiani, M. F.; Kurjiaka, D. T.; Hanes, J.; Shakesheff, K. M.; Goetz, D. J. *Proc. Natl. Acad. Sci. U.S.A.* **2003**, *100*, 15895−15900.
(46) Leckband, D. E.; Schmitt, F. J.; Israelachvili, J. N.; Knoll, W. *Biochemistry* **1994**, *33*, 4611−4624.
(47) Sheth, S. R.; Leckband, D. *Proc. Natl. Acad. Sci. U.S.A.* **1997**, *94*, 8399−8404.
(48) Israelachvili, J. N. *J. Colloid Interface Sci.* **1973**, *44*, 259−272.
(49) Heuberger, M.; Luengo, G.; Israelachvili, J. *Langmuir* **1997**, *13*, 3839−3848.
(50) Derjaguin, B. V. *Kolloid. Z.* **1934**, *69*, 155−164.

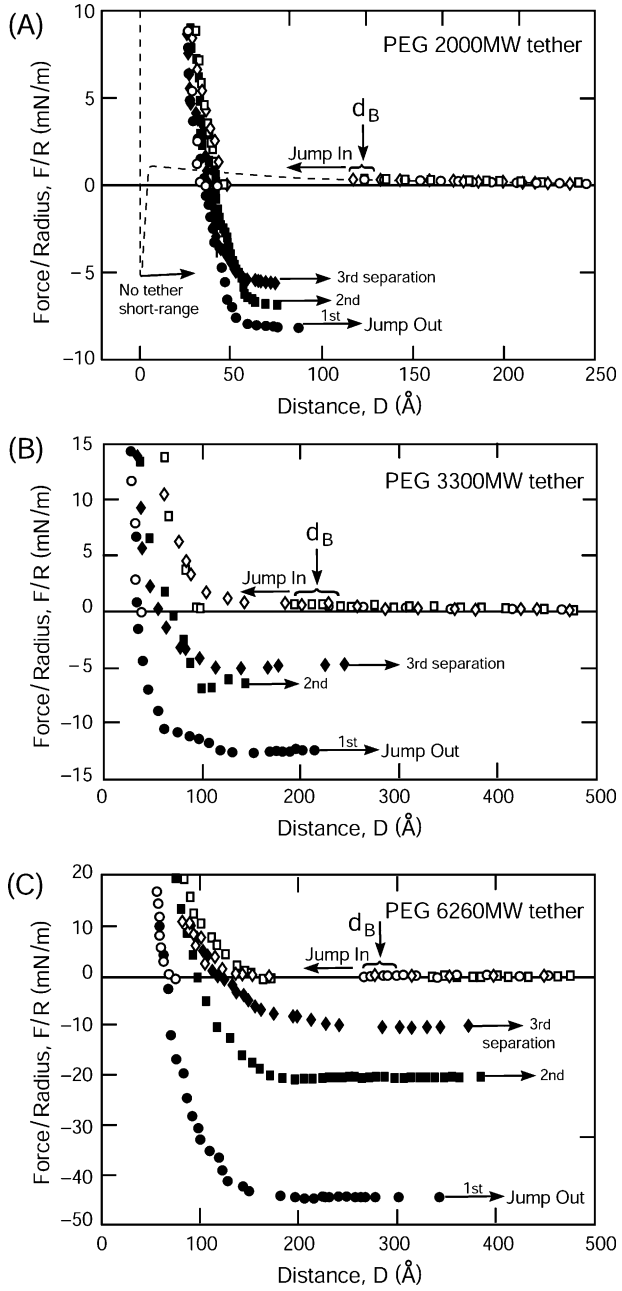

Figure 2. Experimentally measured interaction force profile as a function of separation distance for tethered biotin with an opposing membrane bearing a monolayer coverage of streptavidin. (A) 2000 MW PEG tether, (B) 3300 MW PEG tether, and (C) 6260MW PEG tether. The dashed curve in A shows the short-range interaction between streptavidin with 5 mol % biotin without the PEG tether.[40,42] First approach (○) and separation (●); second approach (□) and separation (■); third approach (◇) and separation (◆). Arrows denote inward and outward jumps on approach and separation, respectively. Force profiles were measured at pH 7.2, 0.5 mM Na^+, and 25 °C (below the phase-transition temperature of the lipid membranes). The arrows indicate the points d_B at which the two surfaces spontaneously "jump" into adhesive contact, which occurs when a sufficient number of biotin groups have bound to the opposing streptavidin receptors and the attractive bridging force of the stretched polymer tethers exceeds the restoring force of the force-measuring spring in the SFA.

governed by the spatial sampling of the tethering chain, resulting in cross bridges at highly stretched conformations.

A quantitative comparison of binding distance for the three PEG tether lengths at constant graft density (Figure 2) reveals that the binding distance d_B at which the ligated tether locks onto the receptor surface increases proportionately with the molecular weight of the tether.[14,17,24] We find a similar dependence of the position of contact (hard wall) with tether molecular weight. It is useful to compare the observed binding distances to the Flory radius, equilibrium brush height, and full extension for each of the tether lengths (Table 1). Because the polymer tether grafting density is kept constant, the lateral overlap of the chains increases with increasing molecular weight. In water, a good solvent for PEG, the increased lateral crowding of the grafted polymer chains leads to an increase in osmotic pressure, causing the chains to stretch away from the membrane into the aqueous phase.

Table 1. Dimensions of PEG Tether Chains and Comparison to Ligand−Receptor Binding Distance

PEG MW	N	R_F (Å)	brush height h (Å)	binding distance d_B (Å)	full extension L (Å)
2000	45	35	37	129 ± 10	160
3300	75	47	61	176 ± 20	265
6260	142	69	116	275 ± 25	500

This average equilibrium extension of the tethering chains from the membrane surface can be estimated using polymer scaling theory for end-grafted chains. Alexander and de Gennes balanced the energetics of the osmotic pressure and elastic resistance to stretching by using the simplest representations of each effect.[51−53] The osmotic pressure, Π, was calculated by assuming a constant density of segments in the polymer layer, which yields the following function

$$\Pi(\sigma, D) \cong \frac{kT}{a^3}\left(\frac{Na^3}{D\sigma}\right) \tag{3}$$

where kT is the thermal energy, D is the extension of the polymer chains from the surface, and σ is the grafting density. The elastic energy per chain was approximated by the energetics of a spring distorted from its mean extension:

$$E(\sigma, D) \cong \frac{kTD}{Na^2}\left(\frac{Na^3}{D\sigma}\right)^{1/4} \tag{4}$$

Hence, the total free energy per polymer chain can be written as

$$E(\sigma, D) \cong kTN\left(\frac{Na^3}{D\sigma}\right)^{5/4} + \frac{kTD^2}{Na^2}\left(\frac{Na^3}{D\sigma}\right)^{1/4} \tag{5}$$

The brush thickness or extension from the surface, h_0, is given by minimizing the free energy

$$h_0 \cong \frac{Na^{5/3}}{\sigma^{1/3}} \tag{6}$$

where all chain ends are localized at the end of the brush. However, these equilibrium calculations do not provide insight into the dynamic conformational sampling of the polymer tether chains, which allow the ligated end to sample the receptor surface at much larger extensions/distances. Consequently, the binding distance would be grossly underestimated from the equilibrium or average extension of the tethers. Experimental results and calculations for the three MW tether chains are summarized in

(51) Alexander, S. *J. Phys.* **1977**, *38*, 983−987.
(52) Degennes, P. G. *Macromolecules* **1981**, *14*, 1637−1644.
(53) Degennes, P. G. *Adv. Colloid Interface Sci.* **1987**, *27*, 189−209.

Table 2. Multivalency of Complementary Binding

PEG MW	binding distance d_B (Å)	average no. of bridging chains at d_B	average no. of ligated chains in the contact region	minimum no. of cross bridges ruptured
2000 1st cnt	134	6.47×10^3	7.9×10^7	1.97×10^6
2000 2nd cnt	133	6.53×10^3		1.66×10^6
2000 3rd cnt	126	1.12×10^4		1.75×10^6
2000 avg	129 ± 10	$(2.0 \pm 1.7) \times 10^4$		2.5×10^6
3300 avg	176 ± 20	6.9×10^4	9.3×10^7	2.5×10^6
6260 avg	275 ± 25	2.1×10^5	1.3×10^8	1.1×10^7

Table 1. In the next section, the characteristic time for a tether chain to sample conformations is estimated.

2. Binding Dynamics. At a simplified level, the polymer tether chain dynamics can be described by modeling the chain as a Hookean spring. Each tether chain will experience fluctuations that allow it to explore a distribution of configurations, including near-full extension. For a particle diffusing in an external potential, $E_{ext}(D)$, the typical exploration time, τ, is given by[54]

$$\tau(D) = \tau_0 \exp\left(\frac{E_{ext}(D)}{kT}\right) \tag{7}$$

If the intrinsic relaxation rate of a single chain, τ_o, is given by the Zimm time,[55]then

$$\tau_0 \approx \frac{\eta {R_F}^3}{kT} \approx 10^{-8}\ \text{s} \tag{8}$$

where η is the viscosity of water. Neglecting lateral interactions between adjacent chains, $E_{ext}(D)$ for $D > R_F$ can be estimated (Hooke's law) by a simple parabolic potential

$$E_{ext}(D) = \frac{(D/R_F)^2 kT}{2} \tag{9}$$

Then, the "typical" exploration time for a 2000 MW PEG chain to sample configurations near full extension is $\tau \approx 10^{-8}$ exp-(12.5) $\approx 10^{-3}$ s; that is, τ is approximately in the millisecond range.

As demonstrated in Figure 2, the biotin at the end of a PEG tether finds a streptavidin binding pocket at a much greater distance compared to the equilibrium extension of the tether for the three chain lengths studied (e.g., 129 ± 10 Å vs 35 Å, respectively, for 2000 MW, Table 1).

This simple analysis qualitatively explains the effect of flexible tethers on the kinetics and spatial range of binding, and a similar type of dynamic interaction potential might be expected to apply to many different types of recognition and specificity. Thus, the tether acts in two manners: (1) it tunes the binding distance and (2) it prevents steric hindrance by raising the ligand away from the membrane surface. Much more precise calculations, which account for the many internal dynamic modes of grafted chains, have been elegantly solved by Moreira and Marques.[22,23]

3. Multivalency and Adhesion. Although single-molecule experiments are important, the geometry in the SFA mimics the multivalency and multiplicity of interactions that are found in vivo. As described in section 1, the measured binding distances d_B are much larger than the equilibrium or average extension R_F of the tethered chains. Initially, each bound chain is stretched and under tension. These bridging chains act as stretched springs linking the two membrane surfaces. When a sufficient number of chains have bound such that the gradient of the total polymer restoring force due to the strongly stretched bridging chains exceeds the mechanical spring constant of the measuring device, the surfaces jump together (Figure 2). The number of chains required to yield this instability can be calculated in a straightforward manner.

In the limit of strongly stretched short chains ($N < 100$), the energy of a polymer tether can be approximated by[22,23]

$$E_{chain} = Nk_BT \log\left[2.15\left(1 - \frac{D}{L}\right)\right] \tag{10}$$

and a corresponding force per chain of

$$f_{chain} = -\left(\frac{\partial E}{\partial D}\right) = \frac{-Nk_BT}{(L - D)} \tag{11}$$

The tensile force exerted by a chain once a bond is formed is then simply calculated with $D = d_B$. The number of chains bound, N_b, at the mechanical instability can be determined from

$$N_b\left(\frac{\partial f_{chain}}{\partial D}\right) = N_b \frac{Nk_BT}{(L - D)^2} \geq k_{sping} \tag{12}$$

A comparison of the measured binding distances, mechanical spring constant, and corresponding number of required bridging chains is provided in Table 2. Significantly, only a small fraction, ~0.1%, of the ligated chains present are required to form cross bridges (tethered ligand−receptor bonds) to exceed the mechanical spring constant and bring the membrane surfaces into close apposition. We observe that subsequent approaches yield a correspondingly lower adhesion as a function of contact/separation cycles as a result of the removal of biotin−PEG−lipid molecules from the membrane (Figure 2). This is not surprising because the membranes are below T_m. In contrast, for fluid-phase membranes, adhesion recovery will occur as a function of the diffusion rate of receptors and tethered ligands.[42,56] A more detailed description of the membrane separation process is discussed next.

4. De-adhesion. Generally, one of three biologically important possibilities arises upon separating ligand−receptor-mediated adhesive membrane surfaces: (i) the ligand−receptor bond breaks, (ii) the ligand anchor is extracted, or (iii) the receptor anchor is extracted. The history of multiple approaches and separations of the ligand and receptor surfaces can be used to elucidate these possibilities. As shown in Figure 2, subsequent approaches yield a correspondingly lower adhesion as a function of contact/separation cycles. In addition, the separation distance at "contact" increases with the number of contact/separation cycles. These findings indicate that the detachment of biotin−PEG−lipid or receptor molecules from the membrane occurs during the separation process.

(54) Truskey, G. A.; Yuan, F.; Katz, D. F. *Transport Phenomena in Biological Systems*; Pearson Education, Inc.: Upper Saddle River, NJ, 2004; p 266.

(55) Rubinstein, M.; Colby, R. H. *Polymer Physics*; Oxford University Press: New York, 2003; p 313.

(56) Helm, C. A.; Israelachvili, J. N.; Mcguiggan, P. M. *Biochemistry* **1992**, *31*, 1794−1805.

The phenomena during membrane separation can be simplified by considering the rupture of a single cross bridge. The force required to break a biotin−streptavidin bond is very high, possibly greater than 130 pN depending on the bond loading rate (binding constant of 88 kJ/mol).[39−41,57,58] However, the force required to extract a lipid anchor from the membrane is significantly less, $f_{lipid} \approx 35$ pN.[59,60] Therefore, the dominant rupture mechanism is expected to be lipid pullout. Many examples of pullout rupture mechanisms exist in cellular de-cohesion.[61,62]

An estimate of the total number of chains involved in the adhesion/decohesion event can be determined by comparing the measured adhesive force upon separating the membranes, F_{ad}, to the force exerted per tethered ligand−receptor bond. Because the lowest-force pathway is that for lipid removal from the membrane, we use this value in the calculation, where N_{cb} is the number of tether cross bridges

$$F_{ad} = f_{lipid} N_{cb} \tag{13}$$

Results from these calculations are provided in Table 2. N_{cb} should always be greater than N_b because additional bonds will be able to form once the surfaces jump into contact. The large variability in the measurements is the result of a number of different factors, including the sensitivity of the polymer tether spring constant to the distances at which the ligand locks into a receptor, contact time, applied load, and approach/separation cycle number.

IV. Discussion

In this work, the binding and adhesion between complementary membranes was investigated. Ligands were placed on flexible polymer chains end-grafted to one membrane, and the other membrane presented complementary receptors. Three polymer tether lengths were investigated. In all cases, the binding of the tethered ligand occurred at highly extended tether conformations. In the case of high-affinity ligand−receptor pairs, as studied here, the binding distance of the ligand−receptor pair was thus governed by the spatial sampling of the flexible tether chains. Only a small fraction of bound, cross-bridging tethers were required to bring the membrane surfaces into physical contact (∼0.1%). Once bonds formed, the attractive bridging force of the stretched polymer tethers pulled the membranes together. As the membranes approached during this process, additional tethered ligand−receptor bonds formed, increasing the number of cross bridges by a factor of up to 1000.

As depicted schematically in Figure 3, the number of accessible receptors increases with the contour length of the tether for curved geometries. Similarly, the length of the tether and the grafting density, if varied, determine the separation distance between the membranes at contact. Closer approach is opposed by the compression of the chains and a concomitant increase in osmotic pressure. For the regions to the right or left of the point of closest approach, the cross-bridging chains at extensions larger than the equilibrium height, h_0, of the grafted tether layer are under tension and result in the measured attractive force between the membranes (Figure 3). In contrast, chains compressed to a thickness below

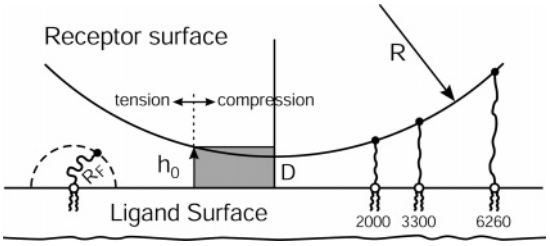

Figure 3. Schematic cartoon of the membranes and curved geometry utilized in the measurements. As the tether chain length increases, the distance at which complementary binding between the two membranes occurs increases. Moreover, a greater number of receptors become accessible, so cross-bridge formation is increased, resulting in higher adhesion. The shaded region defined by the equilibrium height, h_0, of the tether layer defines the regions where cross-bridging chains are under tension or compression.

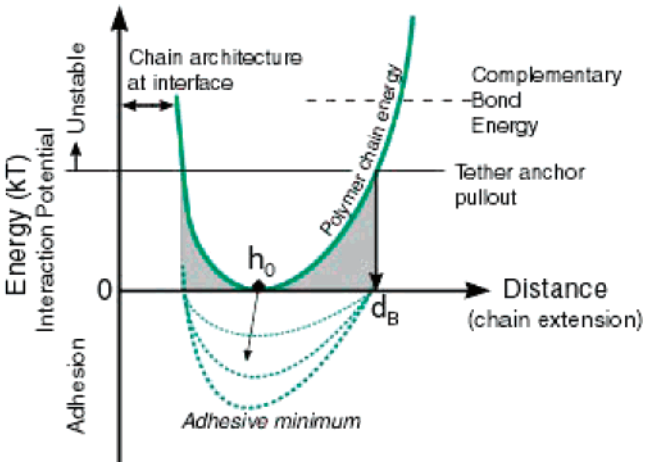

Figure 4. Energy-state diagram for complementary membrane adhesion. The dashed horizontal line is the bond energy of the complementary ligand−receptor pair. The solid horizontal line depicts the lower energy needed to pull a tethered ligand out from the membrane. d_B marks the point on the polymer chain energy curve where the cost of stretching a polymer tether is less than or equal to the weakest link in the system, here the energy to extract a tethered ligand from the membrane. As a result, if a ligand binds a receptor at a distance less than or equal to d_B, then a stable cross bridge can be formed between two membranes. The shaded area defines the region over which stable cross bridges may form. The depth and position of the adhesive minimum (dashed curves) are established by the number of cross bridges, strength of the ligand−receptor binding pair, polymer chain energy, and geometry of the contact area. For curved geometries, the adhesive minimum is located at the distance where the cross-bridge forces of chains under compression or tension are balanced.

h_0 give rise to a repulsive force. The adhesive minimum is located at the distance where these two forces are balanced (Figure 4).

There are multiple modes of failure as the opposing membranes are separated. The streptavidin−biotin ligand−receptor pair is of such high affinity that the primary mechanism is mechanical failure where the lipid-anchored tethered ligands are pulled out from the membrane. As a result, the measured adhesion decreases on subsequent approaches, and the position of contact between the membranes increases. Utilizing micropipet aspiration, Needham and co-workers[16] measured the adhesion between avidin-coated glass beads and lipid microbubbles functionalized with biotin on 3400 MW PEG tethers. They found an adhesive maximum at a concentration of about 5 mol % functionalized lipid, which correlated well with the binding saturation of available receptors. Similarly, adhesive failure was found to be a combination of lipid pullout from the microbubble and ligand−receptor bond failure. No specific adhesion was found when

(57) Evans, E., *Annu. Rev. Biophys. Biomol. Struct.* **2001**, *30*, 105−128.
(58) Merkel, R.; Nassoy, P.; Leung, A.; Ritchie, K.; Evans, E. *Nature* **1999**, *397*, 50−53.
(59) Cevc, G.; Marsh, D. *Phospholipid Bilayers*. Wiley: New York, 1987.
(60) Uster, P. S.; Allen, T. M.; Daniel, B. E.; Mendez, C. J.; Newman, M. S.; Zhu, G. Z. *FEBS Lett.* **1996**, *386*, 243−246.
(61) Bongrand, P. *Physical Basis of Cell-Cell Adhesion*; CRC Press: Boca Raton, FL, 1988; p 267.
(62) Bongrand, P.; Claesson, P. M.; Curtis, A. S. G. *Studying Cell Adhesion*; Springer-Verlag: New York, 1994; p 250.

biotin was on a short spacer or membrane associated in the presence of unfunctionalized PEG chains, as a result of the steric barrier of the PEG layer. More recently, Hammer and co-workers[63] have studied the adhesiveness of polymer vesicles containing functionalized biotinylated polymer to avidin-coated glass beads. Significantly higher adhesion was measured when the biotin was on longer PEG chains, elucidating the impact of steric hindrance on specific binding.

A key feature of the measurements reported here is the determination of binding distances as well as adhesion energies. As shown in Figure 4, although ligands may sample receptors at distances greater than d_B, only bonds that form at energies below the ligand−receptor bond and lipid pullout energies are stable. As a result, binding and the number of possible cross bridges are dependent on the energetics of the tether, the ligand−receptor bond, and the cross-bridging architecture. Although a ligand may sample a receptor pocket at highly stretched tether conformations, stable (to a few kT) cross bridges may form only for energies below the weakest link in the system, in our case, the lipid anchor pullout. On the basis of the measured values of adhesion, up to 20% of the possible cross bridges form on the first contact. This number is reduced with subsequent contacts as more and more cross-bridging tethered ligands are mechanically removed from the membrane upon separation. Typically after three approaches and separations, the interaction is significantly weaker, and little adhesion is measured by the fourth approach, consistent with the number of possible stable cross bridges and the removal of cross-bridging lipid anchors upon separation.

Bell was one of the first to discuss membrane rupture via discrete biospecific cross bridges, and he developed a relationship between the lifetime of cross bridges and the force applied to break the bond. Recently, this work was greatly extended by Evans and co-workers, who measured the strength of single ligand−receptor bonds and determined that bond strength was dependent not only on the force applied but more explicitly on the loading rate of the applied force.[57,58] In contrast to these single-molecule measurements of ligand−receptor bond strength using atomic force microscopy or the bioforce probe, our studies probed the multivalent binding and separation of an ensemble of ligand−receptor-based cross bridges, which precludes the extraction of single-bond properties. It is likely that most biological recognition relies on collective, multivalent binding events such as those described here.

Significantly, although the adhesion decreases with subsequent approaches due to a reduction in the total number of cross bridges formed, the distance at which the membranes jump into physical contact remains the same. This observation indicates that tethered ligands can still easily explore available binding sites even though they have to penetrate through previously removed polymer tethers that are now linked to the receptor membrane surface. This phenomenon may be similar to that for ligands on spacer chains on one cell or a targeted liposome exploring through a target cell's glycocalyx to bind complementary receptors.

In summary, these results suggest that tethered binding kinetics should be considered in detail, and as a process, when describing dynamic bond formation (and dissociation), where the intrinsic binding energy of the adhering molecules is just one of many factors that determine the time evolution of a binding event.

Acknowledgment. This work was supported by NSF NERG DMII-0404457 and DMR-0606564 (T.L.K.) and NIH NHLBI R01 HL72900 (J.Y.W.).

LA702357A

(63) Hiddessen, A. L.; Rodgers, S. D.; Weitz, D. A.; Hammer, D. A., *Langmuir* **2000**, *16*, 9744−9753.